**Egyptian Journal of Geology**
**https://egjg.journals.ekb.eg**

# Geological studies and structural analysis of the Umm Anab metavolcanics and related quartz veins: implications for Pan-African volcanism in the Egyptian Nubian Shield

**Khaled El-Gameel [(1)]*, Sara A. Fayed [(1)], Hamdy A. El Desouky[(2)]** and **Ashraf S. Abdelmaksoud[(1)]**

[(1)] *Geology Department, Faculty of Science, Menoufia University, Egypt.*

[(2)] *Petroleum and mining Geology, Faculty of Science, Galala University*

THE NEOPROTEROZOIC basement complex of the Umm Anab area is located 40 km southwest of Hurghada city in the Northern Eastern Desert (NED) of Egypt. The basement rocks include metavolcanics and enormous plutons of granitoid rocks. The metavolcanics are regionally metamorphosed, forming greenschist to amphibolite facies rocks interbedded with banded iron formation (BIF). Structural analysis in the Umm Anab metavolcanics (UAV) indicates that the area has a poly-phase structural deformation, and each phase has its own effect and style. A Well-developed schistosity striking approximately E-W with dipping 60º-80º southward, and asymmetrical folds with oblique subvertical NNW-striking axial planes were observed. The structural analysis of the veins in metavolcanic by using GArcmB software determined the paleostress inversion and displayed two clusters of veins that formed under two stresses. The stress ratios ($\Phi$)= ($\sigma 2 - \sigma 3$) / ($\sigma 1 - \sigma 3$) for both clusters, respectively, are ~0.39 and ~0.16, which shows two stress status. The values of the stress ratio on vein walls suggest that the host rock was subject to low to moderate tectonic stress at the time the veins formation. In addition, finite strain results in metavolcanics were estimated using the Rf/φ method on deformed pebbles (with a trend of N73º-88ºE), confirming the idea that metavolcanics are affected by low to moderate deformation. The stretching mineral lineation and BIF have trend ENE-WSW to E-W that supports the oldest shortening event (D1) which is considered an early phase of deformation NNW–SSE linked with the Pan-African thrusting.

**Keywords:** Umm Anab, Metavolcanics, Strain analysis, Deformation phases, Egypt, Northeastern Desert.

## 1. Introduction

The research area lies in the northern part of the Arabian-Nubian shield which represents the northwestern segment of the Pan-African orogenic belt and spans vast swaths of NE Africa and the Arabian Peninsula (950-450 Ma; (Kroner, 1984). During the Neoproterozoic, a collection of intra-oceanic island arcs experienced collision and accretion processes and gave rise to the Arabian-Nubian Shield (Kröner, 1991; Ries et al., 1983). During and after the Pan-African events, the Nubian Shield's volcanism and magmatism were significant phenomena (Meneisy, 1990).

Two stages of volcanism have been recognized, the early stage of Pan-African volcanism is represented by ophiolitic and oceanic island arc-related volcanic rocks. The volcanic rocks of this stage were later subjected to low- to medium-grade regional metamorphism, namely metavolcanics (850-620 Ma; (Hashad, 1978; Stern & Hedge, 1985; Meneisy, 1990; Ghareib et al., 2021). The late-stage Pan-African volcanism includes the Dokhan Volcanics, which are mostly subaerial, calc-alkaline, and intermediate to silicic in composition. (639-581 Ma; (El-Ramly, 1972; Dixon, 1979; Stern & Hedge, 1985).

*Corresponding author e-mail: khaled.elgamel@science.menofia.edu.eg
Received: 11/08/2023; Accepted: 05/09/2023
DOI: 10.21608/EGJG.2023.228339.1056

The study area of Umm Anab (Fig. 1) is located 40 km southwest of Hurghada City. It exposes Neoproterozoic basement rocks mainly varieties of volcanic and plutonic rocks. The metavolcanics in Umm Anab area are very important in the NED because they represent few exposures from the early phases of the NED tectonic setting relative to enormous calc-alkaline plutons and subsequent pink post-collision granites. The metavolcanic rocks are predominated in Bir Umm Anab area and have undergone regional metamorphism, typically forming the greenschist to amphibolite facies (El-Tokhi et al., 2010).

Bir Umm Anab area is one of the exceptional places in NED that has island arc metavolcanic interbedded with banded iron formation (BIF). An important feature of the ANS BIF is its Neoproterozoic age as compared to most of the Archean and Early Proterozoic BIF localities all over the world. Eyles & Januszczak, (2004) attributed the BIF in the Neoproterozoic to hydrothermal activity in embryonic rift basins accompanying the breakup of Rodinia. The origin of the Egyptian BIFs remains to be resolved. Previous studies propose that the BIF in Egypt is Neoproterozoic BIF of Pan-African Island arc environment. (El-Gaby et al., 1993; El Habaak & Soliman, 1999; Basta et al., 2000, 2011)

Estimating finite strain in rocks is critical for gaining a comprehensive knowledge of deformational processes and products of all sizes (Kassem et al., 2012). The fracture and vein patterns in the Earth's crust are good indicators for understanding deformational history (D. Koehn et al., 2005). The finite strain in the Umm Anab area, field outcrop photos, and scanned slabs of deformed pebbles in metavolcanic rocks in the study area have been analyzed by the Rf/ϕ method (Ramsay and Huber, 1983). Slabs of metavolcanic rock are cut perpendicular to the foliation and parallel to the mineral elongation (lineation). The Rf/ϕ technique describes clast strain as well as the finite strain found for studied samples (Ramsay and Huber, 1983).

Umm Anab metavolcanics (UAV) received numerous veins, dykes, and off-shoots from the later emplaced activity. Mineral veins are images of fluids venting deep within the earth (Yamaji et al., 2010). The paleostress of dilational fractures has helped us to deduce the stress condition and driving pressure ratio; clustering vein orientations is essential for understanding brittle tectonics (Yamaji et al., 2010; Yamaji & Sato, 2011); moreover, used to deduce the axes of paleostress at the time of the vein formation (Jolly & Sanderson, 1997; Yamaji et al., 2010). The GArcmB software identifies and clusters quartz vein orientations. It estimates stress ratios and axes for each vein group based on the distribution of vein orientations in each group. Furthermore, it may deduce the fluid pressures that dilated these fractures based on the predicted stress distribution on Mohr diagrams (Yamaji et al., 2010; Yamaji & Sato, 2011).

The Umm Anab metavolcanics (UAV) is presented in this article, which will assist shed light on geodynamic history and their genetic ties to the Pan-African volcanism. This study deals mainly with orientation data of dilation veins by overpressured fluids (Baer et al., 1994; Jolly & Sanderson, 1997; Yamaji et al., 2010). The method is based on the fact that fractures open when thermal fluid pressure exceeds the stresses on the fractures (Delaney et al., 1986).

The main target of this paper is to determine finite strain for stretched pebbles, and we estimate paleostress from vein orientations in deformed metavolcanic rocks for the Bir Umm Anab area; also, the study included the relationship between results of finite strain and paleostress; this may lead to understanding the deformational history.

## 2. Geological setting

The investigated metavolcanics are a thick sequence of lava flows that range in composition from basic to acidic with sporadic intercalations of meta-pyroclastic material. The sequence of the metavolcanic forms elongated belt extending from Gabal Hamr and eastward to the main granite pluton of Gabal Umm Anab, acting as ENE= striking belt (Fig. 1). The metavolcanics are intruded sharply by the older granitoids through intrusive contact. The younger granites of Gabal Umm Anab intrude sharply into both metavolcanics and the older granitoids (Fig. 2a). Furthermore both types of granites are sending a large number of dykes and offshoots into the metavolcanics (Fig. 2b).

The Umm Anab metavolcanic rocks are bedded and often dip south at steep angles (dip 50° - 80°), and in some places, they are virtually vertical (Fig. 2c). The studied metavolcanic rocks are sheared and at times exhibit a strong foliation (Fig. 2d). Occasionally, intensive folding are present either onlarge scale or minor scale results in beds repetition (Fig. 2e).

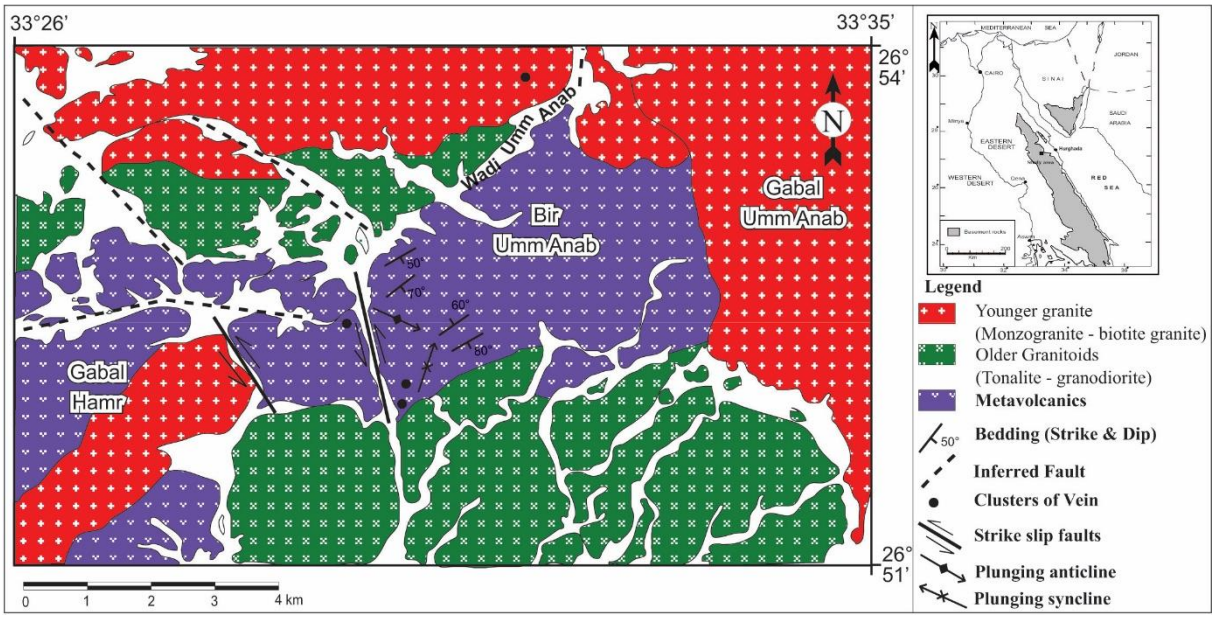


**Fig. 1. Geological map of Bir Umm Anab area, created from Google image mapping and incorporated previous geological information, showing the location map.**

The bedded metavolcanic rocks are intercalated with the iron-formation bands that were observed along the strike and concordant with the metavolcanic's bedding (Fig. 2 f, g). The iron bands are difficult to locate because they vanish beneath the talus or are broken up by dykes. As a result, along the exposures, there are different densities of exposed iron bands. Because they are resistant to weathering, the bands commonly stand as ridges within their host rocks.

Three distinct rock units make up the Umm Anab metavolcanics: basic rocks (amphibolites), intermediate rocks (meta-andesites), and acidic rocks (metafelsites and metarhyolites). Meta-andesites are prevailing rather than the other two types.

The greenschist and amphibolite facies conditions were regionally applied to all units, comparable to the younger meta-volcanics (YMV) (Stern, 1981) of the Central Eastern Desert of Egypt. They exhibit a profusion of porphyritic and more felsic lithologies and a lack of serpentinites.

The later vein intrusion in the metavolcanics is mainly quartz veins. The majority of observed quartz veins are parallel to the foliation trend of the metavolcanic host rocks in concordant aspects. The thicknesses range from 2 cm to 50 cm; the most common orientation of veins is E–W with a dip value between 34° and 88° towards S and W (Fig. 2h).

## 3. Petrography

Umm Anab metavolcanics are massive and fine-grained in hand specimens with reddish grey to dark green in colour. Amphibolite, meta-andesite and metarhyolites are the main types of metavolcanics in Umm Anab area.

### 3.1. Amphibolites

The amphibolites are mostly composed of hornblende and plagioclase, with subordinate quartz. Primary hornblende occurs commonly as porphyroblasts in a fine-grained crystalline groundmass (Fig. 3a). It represents subhedral crystals with pleochroism ranging in colour from yellowish green to green. Tremolite and actinolite as secondary existence of amphibole appear as long prismatic crystals and columnar to fibrous aggregate (Fig. 3b). They occur and form subparallel arrangements either the phenocryst or the groundmass. Most of the amphibole crystals show minor chlorite and epidote alteration.

Plagioclase crystals occur as elongated laths with a composition range from andesine to labradorite (An 35-70). Plagioclase crystals generally show partially

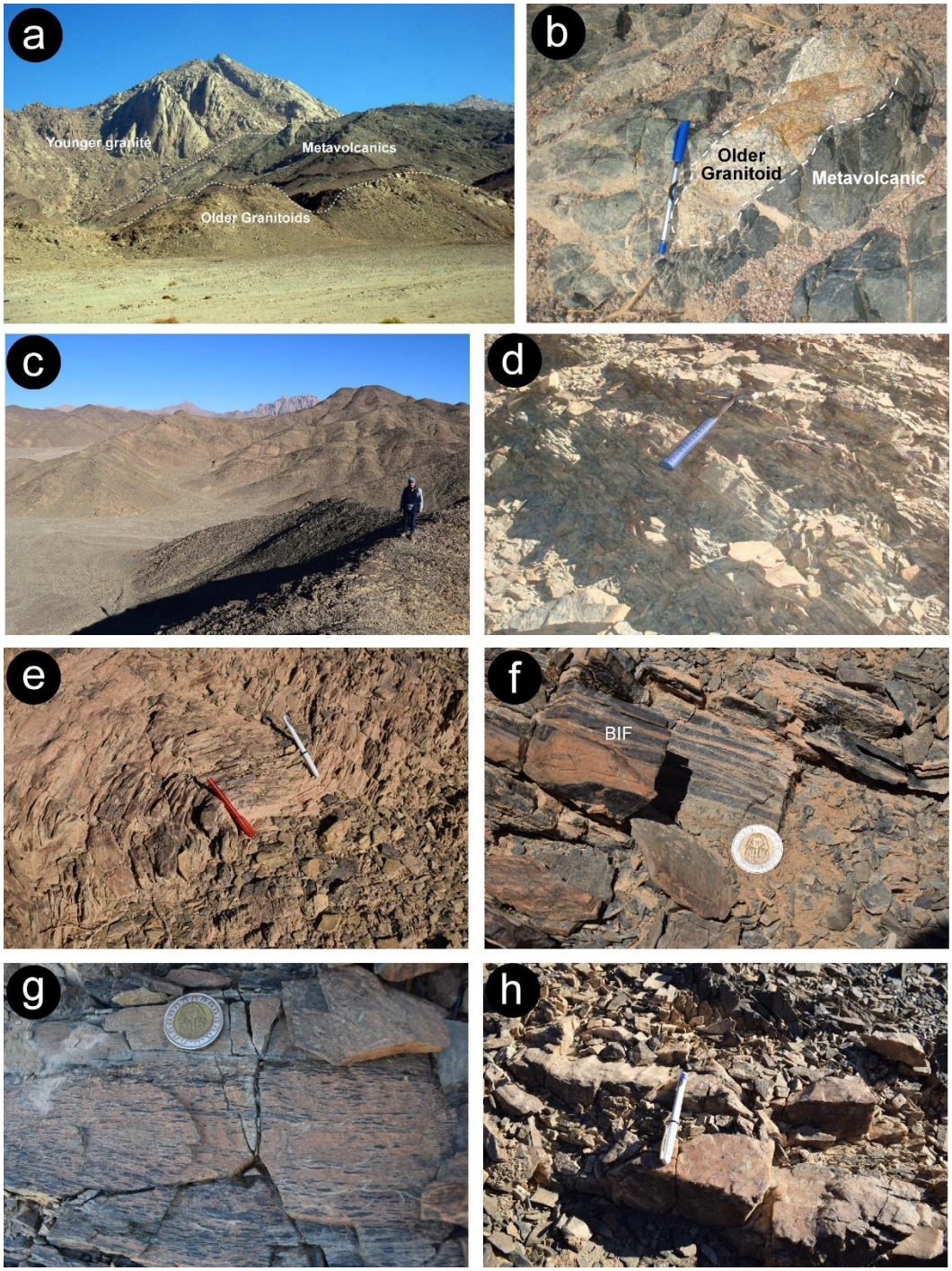


**Fig. 2. a) Field photograph showing the metavolcanic intruded sharply with Older granitoids and both intruded by Umm Anab Younger Granites with sharp contact. Photograph looking Southwest .b) Field photograph showing the offshoots of Older Granitoids in the metavolcanics of Bir UMM Anab area, photograph looking West. c) Field photograph of Bir Umm Anab Metavolcanics showing the dipping towards North and South, looking West. d) Field photograph of Metavolcanics in Bir Umm Anab showing schistosity, looking Southwest. e) Minor folds with axial plane strike in SSE and developed during D2 deformational phase; photograph looking NNE. f) Banded Iron Formation (BIF) intercalated with metavolcanic, Photograph looking East. g) Mineral lineations moderately to steeply plunging towards E-W and developed during D1 deformational phase; Photograph looking South. h) Field photograph of the E–W oriented veins with a dip value of 83° towards S; Photograph looking South.**

to completely saussuritization and sericitization processes resulted in secondary epidote and sericite minerals. Augite mineral occurs as subhedral crystals that are commonly cracked and altered to fibrous actinolite and chlorite. Quartz is present in small amounts filling interstitial spaces between the other constituents. Accessory components are apatite, zircon and iron oxides. Apatite occurs as

short prisms or minute needles enclosed in plagioclase crystals.

The amphibolites occur mostly in aphanitic to porphyritic texture and show degrees of schistosity. Minor folding is commonly observed in thin-section of amphibolite (Fig. 3c). Also foliation and lineation in the same direction is observed. Microveins of quartz and calcite are present as late-stage filling and follow the same direction of foliation and lineation (Fig. 3d).

The iron oxides (BIF) form irregular grains and occur in random distribution but mostly tend to be banded in subparallel arrangement (Fig. 3e). The BIF in Um Anab area belongs to the oxide facies (Basta et al., 2011). The oxide facies bands are composed mainly of iron oxide mesobands alternating with chert or jasper mesobands. The iron oxide mesobands are composed essentially of magnetite, usually less abundant hematite and microcrystalline quartz.

### 3.2. Meta-Andesites

Meta-andesites are composed mainly of plagioclase, hornblende and biotite. The plagioclase crystals are mainly andesine and oligoclase (An 15- 25). Hornblende shows moderate pleochroism from yellowish green to dark green and often contains apatite and iron oxide inclusions. Biotite is present as fine flakes (up to 0.2mm) disseminated among the other minerals. It is commonly altered to chlorite along the cleavage planes. Quartz occurs as subhedral crystals (up to 0.2 mm across) and as fine-grained aggregates scattered throughout the groundmass and fill several voids. Accessory minerals are Zircon, apatite and opaques. Actinolite, epidote, zoisite, sericite and chlorite are secondary minerals in the meta-andesite rocks and could give an indication of low-grade greenschist facies.

The meta-andesite occurs as fine grained aphanitic and other porphyritic varieties. Schistosity and lineation are not common compared to the amphibolite samples.

### 3.3 Metarhyolites

Metarhyolites are the acidic variety of metavolcanic in Umm Anab area. They are light coloured and composed mostly of quartz and plagioclase feldspar (Fig. 3f). Plagioclase is mostly subhedral crystals of oligoclase (An 15-25) which are partially alterated to sericite. Accessories are biotite, zircon, apatite and iron oxides. The quartz and plagioclase phenocrysts are clustered to form glomeroporphyritic texture.

Varieties of metarhyolites are aphanitic and occasionally host aggregates of quartz crystals as euhedral microphenocrysts that represent late-stage filling voids. So, these secondary quartz crystals do not show any degrees of deformation.

## 4. Structural setting

According to a field study of structural elements observed in the Neoproterozoic crystalline basement, (Hamimi et al., 2018) mentioned three deformation events that influenced the Egyptian Eastern Desert: syn-accretion phase (D1), post-accretion phase (D2), and a long-lasting extensional phase (D3). The structural field measurements and overprinting relations observed in the Bir Umm Anab area revealed two main deformational events (D1 and D2). The two detected deformational phases from measurements of linear elements and minor folds. The following section explains the two events and related structures in the metavolcanic.

### 4.1. Phases of Deformation

The D1 deformation phase (NNW–SSE shortening) is the first event to influence metavolcanic in the study area. The NNW–SSE shortening spreads over the Eastern Desert of Egypt and is associated with oblique island arc accretion (740–680 Ma) (Greiling et al., 1994). It is responsible for the (S1) schistosity (ENE–WSW striking with dipping 60º-80º mainly to the SSE but sometimes changed to the NNW) with mineral lineations (L1) running in metavolcanic with a nearly E-W trend and plunges 27º-65º to the west but occasionally to the east (fig. 2g). The lineations (L1) (as oriented deformed pebbles) are seen and preserved in the metavolcanic with a nearly E-W trend of the long axes parallel to the structures formed during the first phase of deformation (D1). Foliation (S1) constitutes minor overturned folds (F1), with the strike of the axial plane into N67ºE and dipping moderately into 48º.

Structures that emerged later in the orogeny, when East and West Gondwana met and the Arabian Nubian Shield was squashed between them, constitute the second deformational event or D2 (Abdeen & Abdelghaffar, 2007; Johnson & Woldehaimanot, 2003; Kusky, 2003). The D2 deformation (compression and shortening) is the second event that influences metavolcanic. The D2 structures observed in the metavolcanic are NNW-

SSE trending according to the effect of the second phase deformation. The orientation of schistosity (S2) is changed and produces minor asymmetrical folds (F2) with oblique axial planes striking into the (NNW-SSE) and dipping steeply 85º (fig. 2e). The mineral lineations (L1) were generated during the (D1) deformation phase, later affected by the second phase (D2); its trend (L2) changed to N25ºW with steeply descending planes and parallel to the minor fold axes (F2).

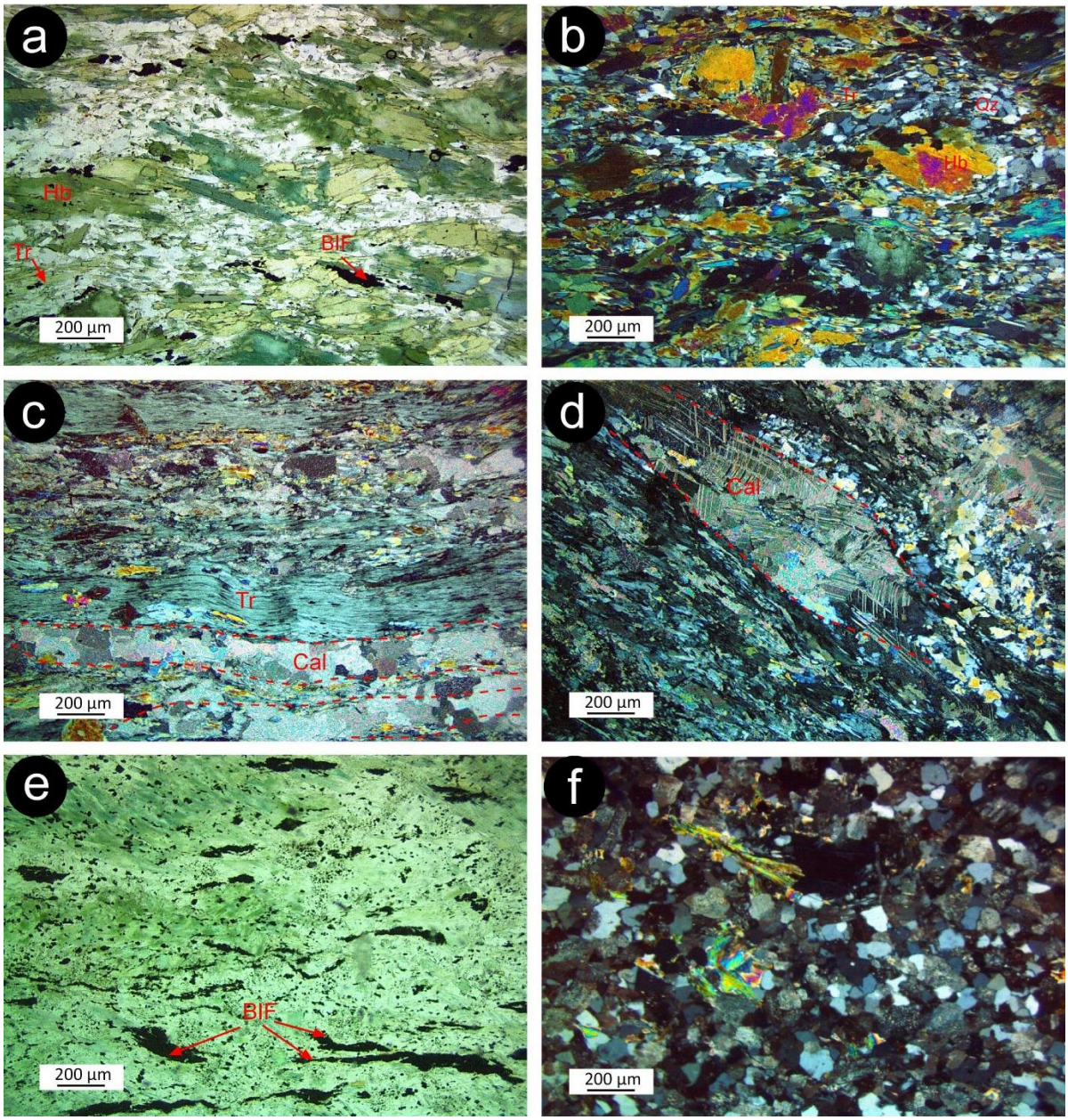


**Fig. 3. a) photomicrograph showing the alignment of amphibole crystals in amphibolite rock., b) photomicrograph showing simple twinning in hornblende (Hb), long prismatic crystals and columnar to fibrous aggregate of tremolite (Tr). c) Photomicrograph showing folding in tremolite, and veins with different thickness concordant with the foliation direction. d) Photomicrograph showing veins of calcite in metavolcanics (amphibolite). e) Photomicrograph showing Banded Iron Formation BIF., f) Photomicrograph showing the felsic component of metarhyolite.**

## 5. Paleostress analysis of vein orientations

### 5.1. Data acquisition

The data analysis deals with vein orientations, so orientation data from 151 veins were collected in the present study. The analyzed datasets were mixed Bingham distribution using GArcmB software (Yamaji, 2016) for deducing paleostress inversion. A method of Bingham distribution is recognized with the concentration of axes (Love 2007), in which the maximum ($\sigma 3$), intermediate ($\sigma 2$), and minimum ($\sigma 1$) concentration axes (Baer et al., 1994). The Mixed Bingham distribution method is used for the vein orientation; the axes of each Bingham component are described as the principal axes of the paleostress at the time of vein formation. Moreover, the stress ratios are determined from concentration parameters(Yamaji & Sato, 2011), in which the method postulates that veins are formed from a fluid of various pressures.

### 5.2. Results

The results of the analysis of the veins are shown in the figure. 4 (a, b) as two clusters (*K*) of vein that formed under two stresses, called UA and UB, the minimum value of the Bayesian information criterion (BIC) was recorded (326.109) from the attitudes of veins that dilated the metavolcanic layers when the number of clusters (*K*) was two (Fig. 4a). Memberships of veins are marked with small circles, as in Fig. 4b; in the stereogram, the black circles suggest that the veins probably formed under stress UA, while the open and coloured circles indicate veins under stress UB. The UA and UB stresses were marked with the mixing coefficient ($\varpi$) values of 0.32 and 0.68, respectively (Fig. 5a, 5b). In which the stress ratios ($\Phi$)= ($\sigma 2 - \sigma 3$)/($\sigma 1 - \sigma 3$) for both clusters, respectively, are ~0.39 and ~0.16, which shows a two-state of stress (Fig. 4b).

The first characterized cluster shows SE oblique $\sigma_1$ (dip direction/dip: 152.2°/35.7°), W oblique $\sigma_2$ (263°/26.3°), and NE oblique $\sigma_3$ (020°/42.9°) in which the second cluster shows W horizontally $\sigma_1$ (268°/2.9°), NE vertically $\sigma_2$ (029.3°/84.4°), and S horizontally $\sigma 3$ (177.7°/4.8°). If $p_f$ is fluid pressure, then $p = (p_f - \sigma_3)/(\sigma_1 - \sigma_3)$ is the 'driving pressure ratio' (Baer et al., 1994); the $p^*$, in Figure 4a, b indicates the lower bound of the *P* values of the veins, yielding $p^* \leq$ ~0.11 and $\leq$ ~0.23 for the two clusters (Fig. 4a, b).

## 6. Finite-strain analysis

### 6.1. Methods

Finite strain (*Rs*) analysis was determined from aggregates in deformed rocks with several methods (Hamimi et al., 2014; Kassem et al., 2012). Our study used the *Rf*/$\varphi$ method for twelve samples collected from the metavolcanic rocks at Bir Umm Anab (Tables 1, 2), to calculate two-dimensional finite strain for stretched pebbles in deformed metavolcanic rocks at Bir Umm Anab, Eastern Desert. The technique of the *Rf*/$\varphi$ is based on the determination of the ratio of the long axis and short axis (*Rf*) and orientation ($\varphi$) for constructing the *Rf*/$\varphi$ diagram for matching them with (LISLE , 1985) standard strain curves to elliptical or sub-elliptical shapes of deformed aggregates (Mulchrone & Meere, 2001; Ramsay J. G. and Huber M. I., 1983; Wallbrecher, 2012), are the most accurate computer software used recently to calculate finite strain with the *Rf*/$\varphi$ method after enhancements over the years by authors such as (Dunnet, 1969; LISLE, 1985, Kassem et al., 2012).

The Macromedia FreeHand MX 11 was used to trace the outlines of deformed pebbles and produce a digital file (BMP file) for each image taken from outcrops in a field and a scanned photo of the hand specimen slabs. Samples of metavolcanic rock cut parallel to mineral elongation (lineation) and perpendicular to the foliation. Digital image processing by (Mulchrone et al., 2005) Semi-Automatic Parameter Extraction program (SAPE) to obtain strain parameters from grain boundary traces of deformed pebbles in metavolcanic. These parameters are long axis (a), short axis (b), (*Rf*) axial ratios of typically between 40 and 105 strain markers, and ($\varphi$) data along the line of maximum

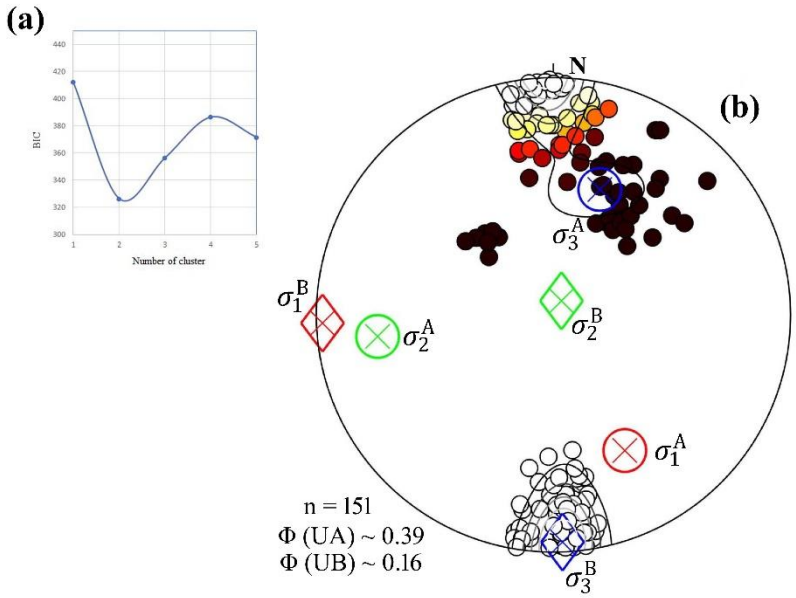


**Fig. 4. Stress analysis of veins in Bir Umm Anab metavolcanic. (a) According to the minimum Bayesian Information Criterion (BIC) at the number of clusters (N) K=2, the vein orientations are divided into two clusters that lead to two corresponding stresses called Stresses UA and UB. (b) The lower hemisphere, equal-area projection of poles to veins, and the concentrations of principal axes are determined from the veins' orientations by Yamaji and Sato's (2011) method.**

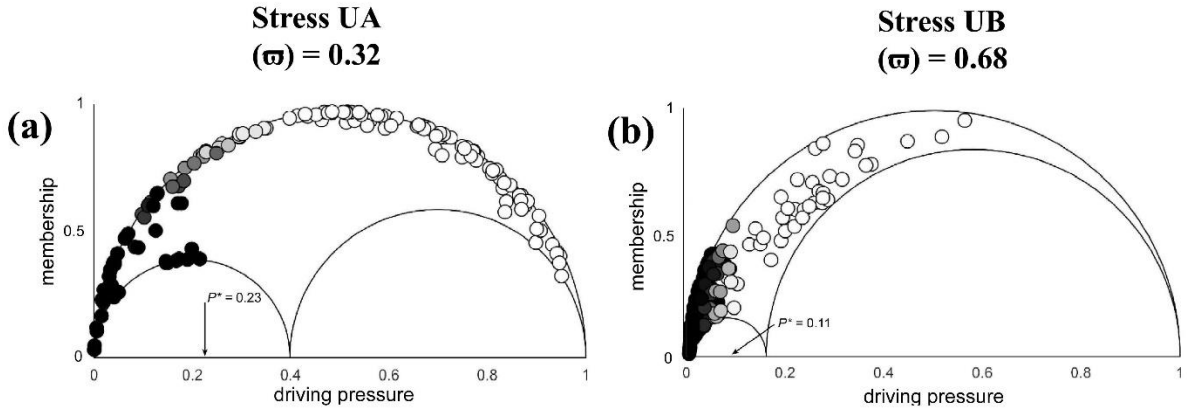


**Fig. 5. Mohr circles of the stresses evaluated on the vein walls and the resulting fluid pressures. (a) Fluids pressures of the first cluster passed through fractures of the metavolcanic equal 0.23. (b). And the fluid pressures of the second cluster equals 0.11.**

stretching orientation extracted from the BMP image by SAPE.

For producing the *Rf*/*φ* diagrams to determine finite strain, (Chew, 2003) spreadsheet (CSS) is used. The spreadsheet consists of four worksheets, entering the strain parameters as long and short axes (a), (b), (*φ)*, and (*Rf*), respectively, in the first "Enterdata" sheet. Only export parameters as *Rf*/*φ* from the SAPE program and save data as (RFP) file extension, which aids in calculating finite strain when importing them into (Mulchrone et al., 2003) MRL (Mean Radial Length) software.

### 6.2. Results

The outputs of strain estimation of deformed pebbles in metavolcanic rocks in three observed locations are tabulated in Table 1 and graphically presented in Figs. 6–10. The results of finite strain for the Rf/ϕ method are recorded from CSS between 1.23 to 1.73 for deformed metavolcanics

rocks (Figs. 6-8-10). The results recorded from the strain analysis from the CSS and MRL programs are closely harmonious and symmetrical (Table 1). The obtained values of vector mean, harmonic mean, Ln harmonic mean, index of symmetry ($I_{SYM}$), Chi-square ($x^2$), and *R*s from the CSS (Table 2).

The $I_{SYM}$ levels in this study's $Rf/\varphi$ based-methods samples are often greater than Lisle's (1985) critical values, in which the $x^2$ values computed using the CSS program on deformed pebbles in metavolcanic rocks at Bir Um Anab demonstrate that the samples had $x^2$ values lower than (LISLE, 1985) critical $x^2$ values. The $I_{SYM}$ values decide whether the distribution of strain data is symmetrical or asymmetrical. The minimum $x^2$ value is another essential parameter to check the initial orientation of the markers before deformation after calculating the finite strain (Chew, 2003; LISLE, 1985; Mulchrone & Meere, 2001).

**Table 1. The average MRL strain data for the observed and analyzed deformed pebbles in metavolcanics from three locations is shown below.**

| Method | Rs (lower) | Rs | Rs (upper) | $\varphi$ (lower) | $\varphi$ | $\varphi$ (upper) |
|---|---|---|---|---|---|---|
| **A: The average of MRL strain data for four samples of deformed pebbles in metavolcanics from location 1.** | | | | | | |
| **Mulchrone et al (2002)** | 1.72 | 1.81 | 1.91 | -11.91 | -9.83 | -7.97 |
| **Robin (1977)** | 1.70 | 1.78 | 1.87 | -13.06 | -10.87 | -8.63 |
| **Robin & Torrence (1987)** | 1.73 | 1.78 | 1.83 | -13.06 | -10.87 | -8.63 |
| **Mulchrone & Meere (2001)** | 1.60 | 1.70 | 1.95 | -12.92 | -10.87 | -8.59 |
| **Yu and Zheng (1984)** | 2.39 | 3.37 | 5.98 | -12.71 | -10.87 | -8.73 |
| **Harmonic Mean** | 1.82 | 1.90 | 1.99 | N/A | N/A | N/A |
| **Geometric Mean** | 1.97 | 2.07 | 2.18 | N/A | N/A | N/A |
| **Arithmetic Mean** | 2.17 | 2.29 | 2.43 | N/A | N/A | N/A |
| **Mulchrone (2004)** | 1.72 | 1.81 | 1.90 | -11.92 | -9.83 | -7.75 |
| **A: The average MRL strain data for five samples of deformed pebbles in metavolcanics from location 2.** | | | | | | |
| **Mulchrone et al (2002)** | 1.57 | 1.67 | 1.78 | -89.72 | 87.74 | 89.79 |
| **Robin (1977)** | 1.57 | 1.67 | 1.78 | 84.05 | 87.10 | 90.28 |
| **Robin & Torrence (1987)** | 1.61 | 1.67 | 1.73 | 84.05 | 87.10 | 90.28 |
| **Mulchrone & Meere (2001)** | 1.50 | 1.75 | 1.85 | 84.03 | 87.10 | 90.52 |
| **Yu and Zheng (1984)** | 1.86 | 2.54 | 4.68 | -89.10 | 87.10 | 89.52 |
| **Harmonic Mean** | 1.96 | 2.05 | 2.17 | N/A | N/A | N/A |
| **Geometric Mean** | 2.14 | 2.25 | 2.38 | N/A | N/A | N/A |
| **Arithmetic Mean** | 2.35 | 2.49 | 2.64 | N/A | N/A | N/A |
| **Mulchrone (2004)** | 1.50 | 1.67 | 1.83 | 84.27 | 87.74 | 91.21 |
| **A: The average MRL strain data for three samples of deformed pebbles in metavolcanics from location 3.** | | | | | | |
| **Mulchrone et al (2002)** | 1.21 | 1.30 | 1.40 | 7.94 | 15.37 | 23.65 |
| **Robin (1977)** | 1.20 | 1.29 | 1.38 | 9.43 | 19.66 | 29.26 |
| **Robin & Torrence (1987)** | 1.22 | 1.29 | 1.36 | 9.43 | 19.66 | 29.26 |
| **Mulchrone & Meere (2001)** | 1.10 | 1.15 | 1.40 | 9.91 | 19.66 | 29.35 |
| **Yu and Zheng (1984)** | 1.20 | 1.59 | 2.64 | 9.87 | 19.66 | 29.97 |
| **Harmonic Mean** | 1.75 | 1.84 | 1.94 | N/A | N/A | N/A |
| **Geometric Mean** | 1.88 | 1.99 | 2.11 | N/A | N/A | N/A |
| **Arithmetic Mean** | 2.04 | 2.18 | 2.34 | N/A | N/A | N/A |
| **Mulchrone (2004)** | 1.21 | 1.30 | 1.39 | 7.67 | 15.37 | 23.06 |

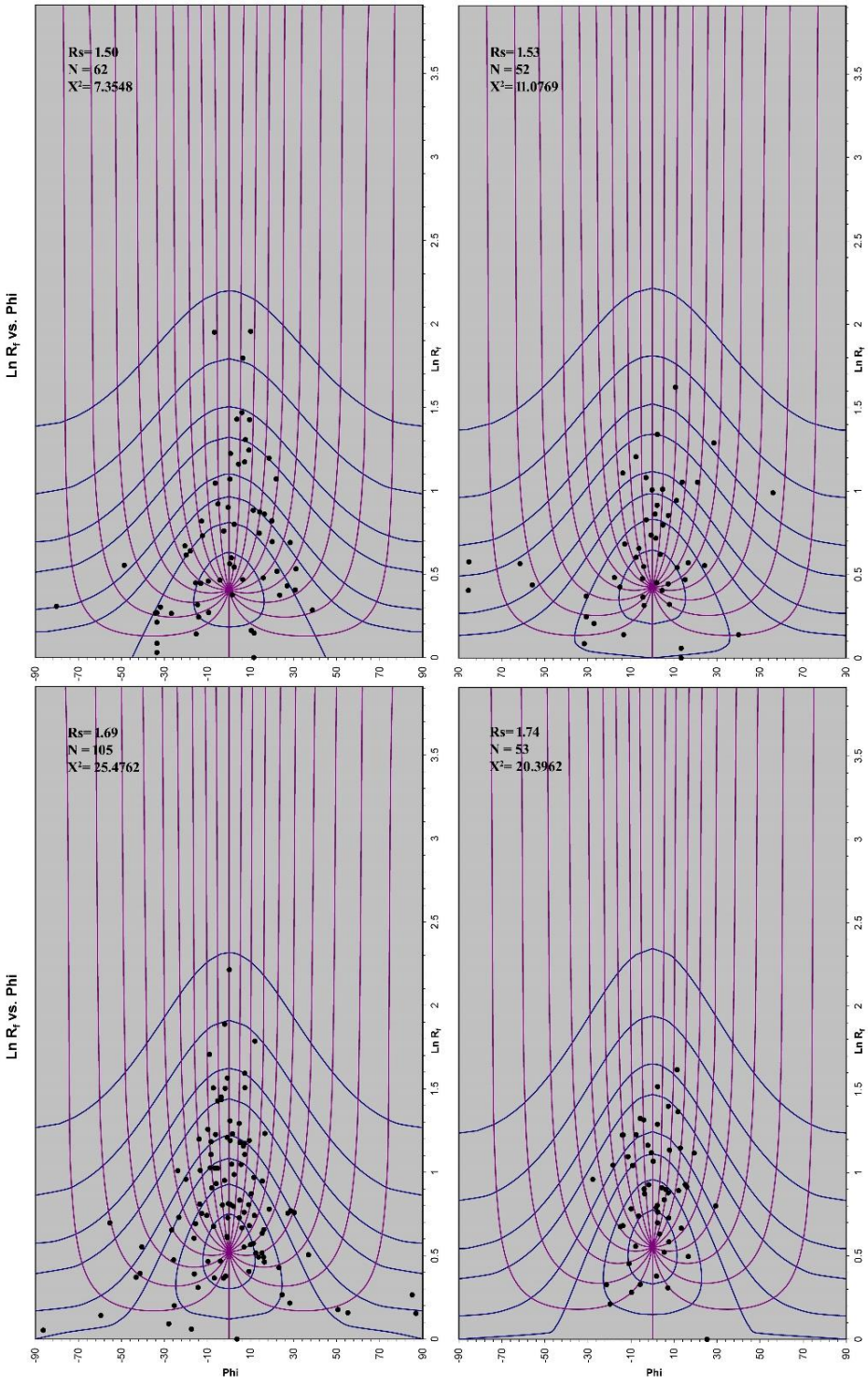


**Fig. 6. RF/φ plots show the strain ratios of four samples (1 to 4) of metavolcanic rocks (L1) in the study area (Lisle, 1985).**

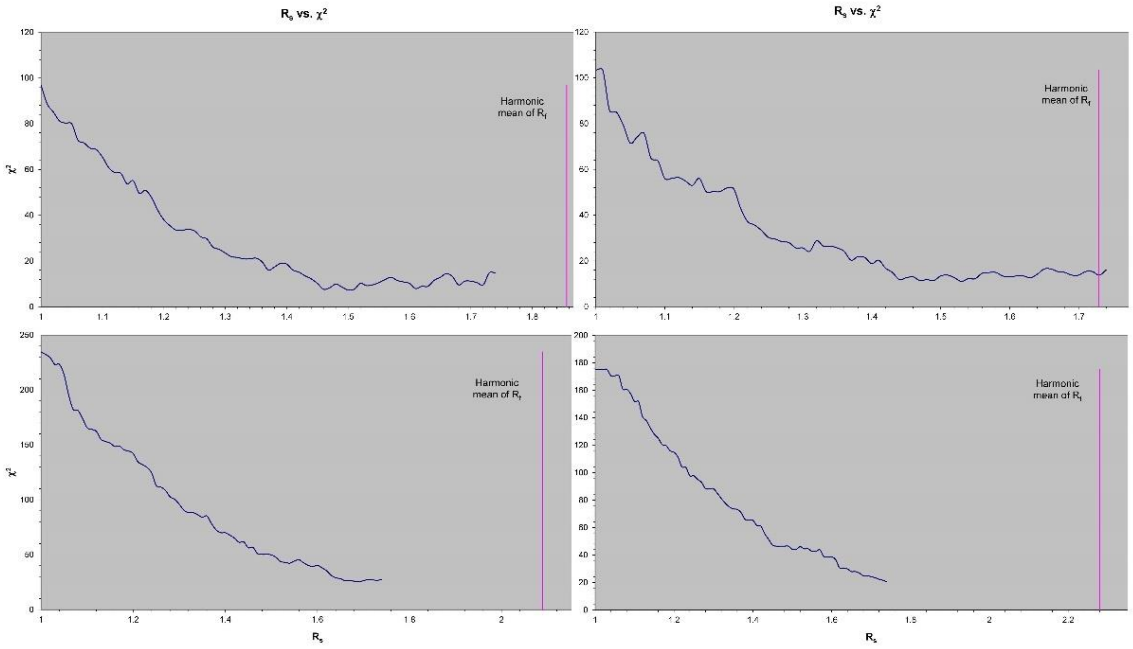


**Fig. 7. Plotting of Rs vs. X2 showing how the strain (Rs) affects the best-fit parameters (X2) of θ-distribution text in the Bir Umm Anab of the previous four samples (1 to 4).**

## 7. Discussion

During the Pan-African Orogeny, the metavolcanic rocks in the study region underwent two deformation events: the oldest (D1) and the youngest (D2). The shortening event (D1) is considered an early phase of deformation NNW–SSE shortening event linked with Pan-African thrusting (Abdelsalam et al., 2003; Stein & Goldstein, 1996; Stern, 1994). During this phase, a well-developed schistosity (S1) that strikes from (ENE-WSW to E-W) with dipping 60º-80º towards the south was formed. In foliation, a good indication supporting the D1 event (NNW-SSE), in which the stretching mineral lineations (L1) as oriented deformed pebbles have a trend (ENE-WSW to E-W).

The studied finite strain (*Rs*) from deformed pebbles (with a trend N73º-88ºE) that deformed during the first phase of deformation (D1). The highest values of $I_{SYM}$ reveal that the strain data distribution is symmetrical and uniform and supports the concept of random marker orientation before deformation (Table 2). The low $x^2$ values obtained from the CSS software support the idea that the markers had no original preferred orientation before deformation (random orientation), and average strain analysis results from CSS and MRL software indicate that the area is affected by a low to moderate deformation (Tables 1 & 2 and Figs. 6–10).

As a result of increasing the deformation, overturned folds (F1) formed in metavolcanic with an axial plane semi-parallel to the orientation of the foliation as (N67ºE). From the field measurements, we observed a small amount of the deformed pebbles and stretching mineral lineations enclosed within the metavolcanic with a new orientation (S20º-35ºE), probably resulting from the impact of the (D2) second phase of deformation (ENE-WSW), to produce (L2). With the compression of this phase of deformation (D2), asymmetrical folds with oblique (NNW-SSE) oriented axial planes are created, with the concurrent creation of two clusters of fractures, from minor ones (WNW-ESE) to a majority (E-W) oriented.

Our optical microscope observation shows a different thickness of fractures along the folding; fractures were filled with blocky equidimensional quartz grains and dilated to produce veins (Fig. 3c). Figure. 4 (a, b) displays two clusters of vein that formed under two stresses, UA and UB. According to the (ϖ) values shown in (Fig. 5a, 5b), the vein formed 32% under-stress UA and 68% under stress UB. Under the stress condition (UB ), a strike-slip tectonic faulting regime with a nearly vertical σ2-

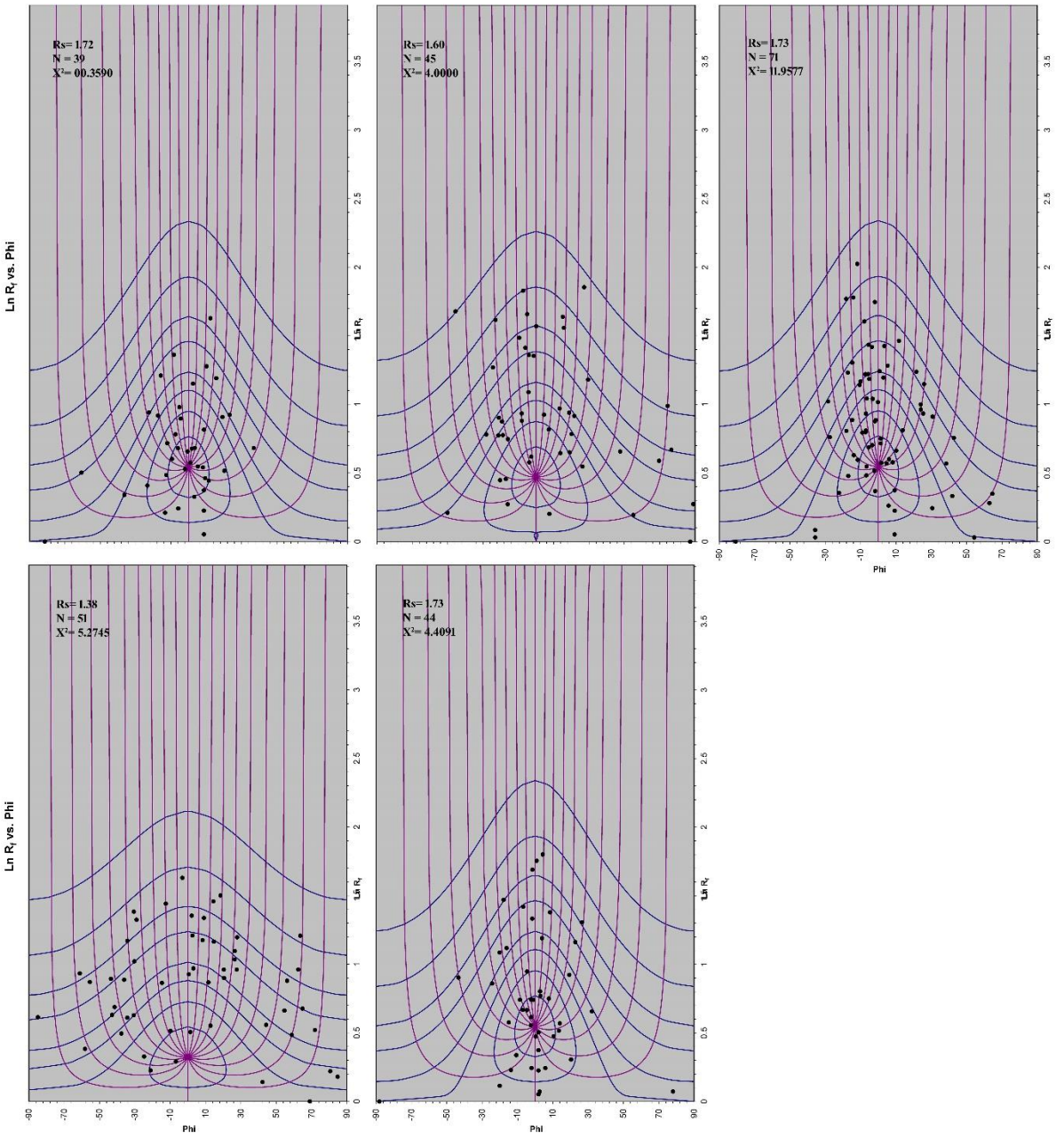


**Fig. 8. RF/φ plots show the strain ratios of five samples (5 to 9) of metavolcanic rocks (L2) in the study area (Lisle, 1985).**

axis formed the majority of veins (68%). The rest of the studied formed veins (32%) underwent stress under the stress condition (UA ), a normal faulting tectonic with a nearly oblique three-axis. The (UA and UB) affected the area as normal faulting and strike-slip tectonic regimes, responsible for forming veins that dilated the metavolcanic foliations. The veins yielded N–S extensional stresses with low-stress ratios for all veins, ranging from ~0.39 and ~0.16 (Fig. 4b). Moreover, studying a thin section clast of hornblende in a matrix of quartz shows σ – type with dextral shear sense (Fig. 3b), in which the quartz grains aggregate, probably formed by dynamic recrystallization. The σ -type is a shear criterion indicating creation at the lower strain (Passchier, 2005), which is compatible with the

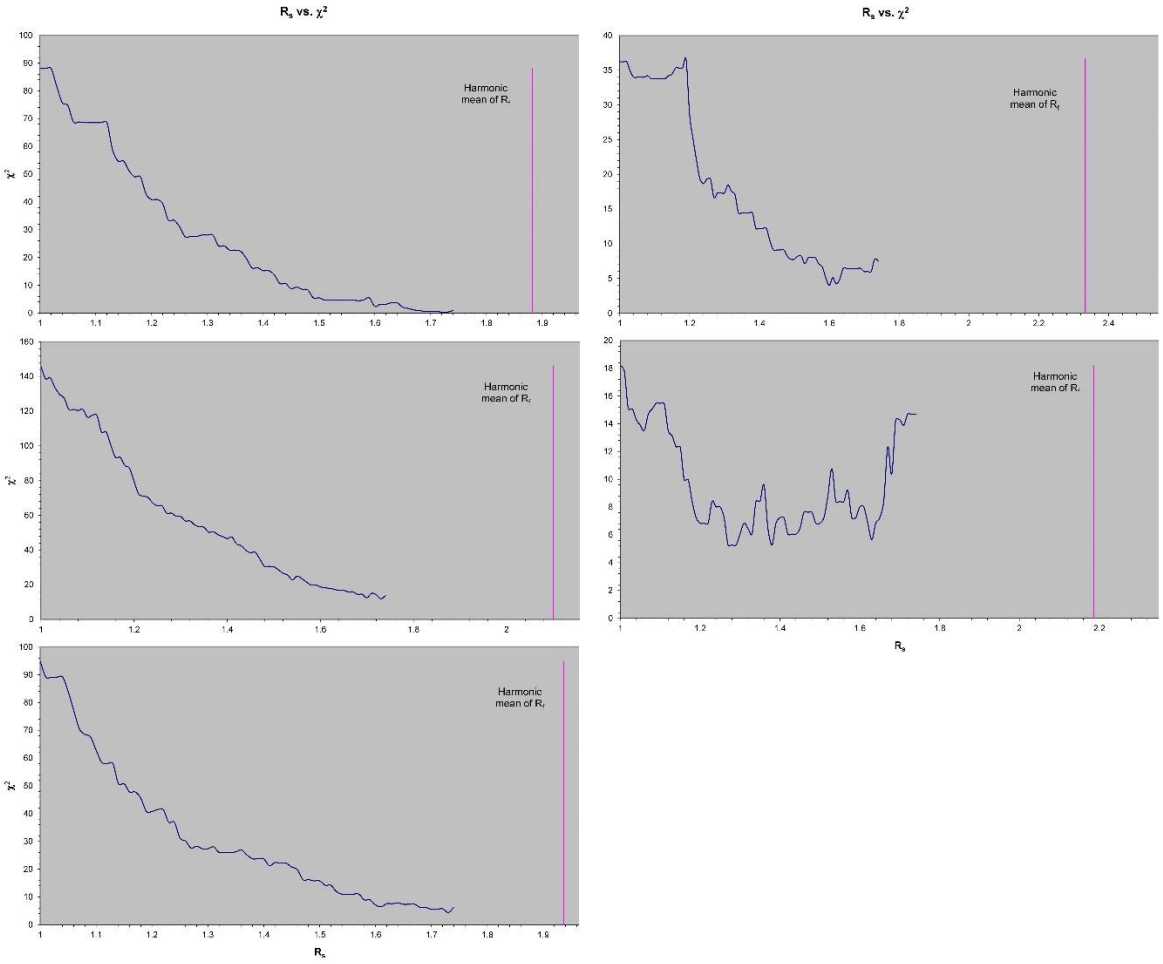


**Fig. 9. Plotting of *Rs* vs. $X^2$ showing how the strain (Rs) affects the best-fit parameters ($X^2$) of θ-distribution text in the Bir Umm Anab of the previous five samples (5 to 9).**

lower stress ratios ($\Phi$) obtained from vein analysis (Fig. 4b). Finally, the weak extensional stresses resulting from vein analysis are not sufficient to cause deformation in the host rocks so the most fixed orientation of deformed pebbles has resulted from the impact of the first event to influence metavolcanic in the study area as a shortening deformation phase (NNW–SSE).

## 8. Conclusion

Bir Umm Anab area is located 40 km southwest of Hurghada city and represents excellent outcrops of Neoproterozoic basement complex in the northeastern Desert (NED). The basement outcrops are mainly metavolcanics intruded by several types of granitic rocks. Concerning the metavolcanics in this study the geological affinity and the structural analysis are quite important since the metavolcanics are not common in the NED relative to the post-collision granitoids.

The investigated metavolcanics form elongated belt extending from Gabal Hamr and eastward to the main granite pluton of Gabal Umm Anab and represent a thick sequence of lava flows that range in composition from basic to acidic with sporadic intercalations of meta-pyroclastic material. The sequences of Umm Anab metavolcanics are intercalated with banded iron formation (BIF) and form bedded sequences dipping south at steep angles or vertically in some parts.

The studied metavolcanic rocks are sheared and at times exhibit a strong foliation with intensive folding in some locations either on large or minor

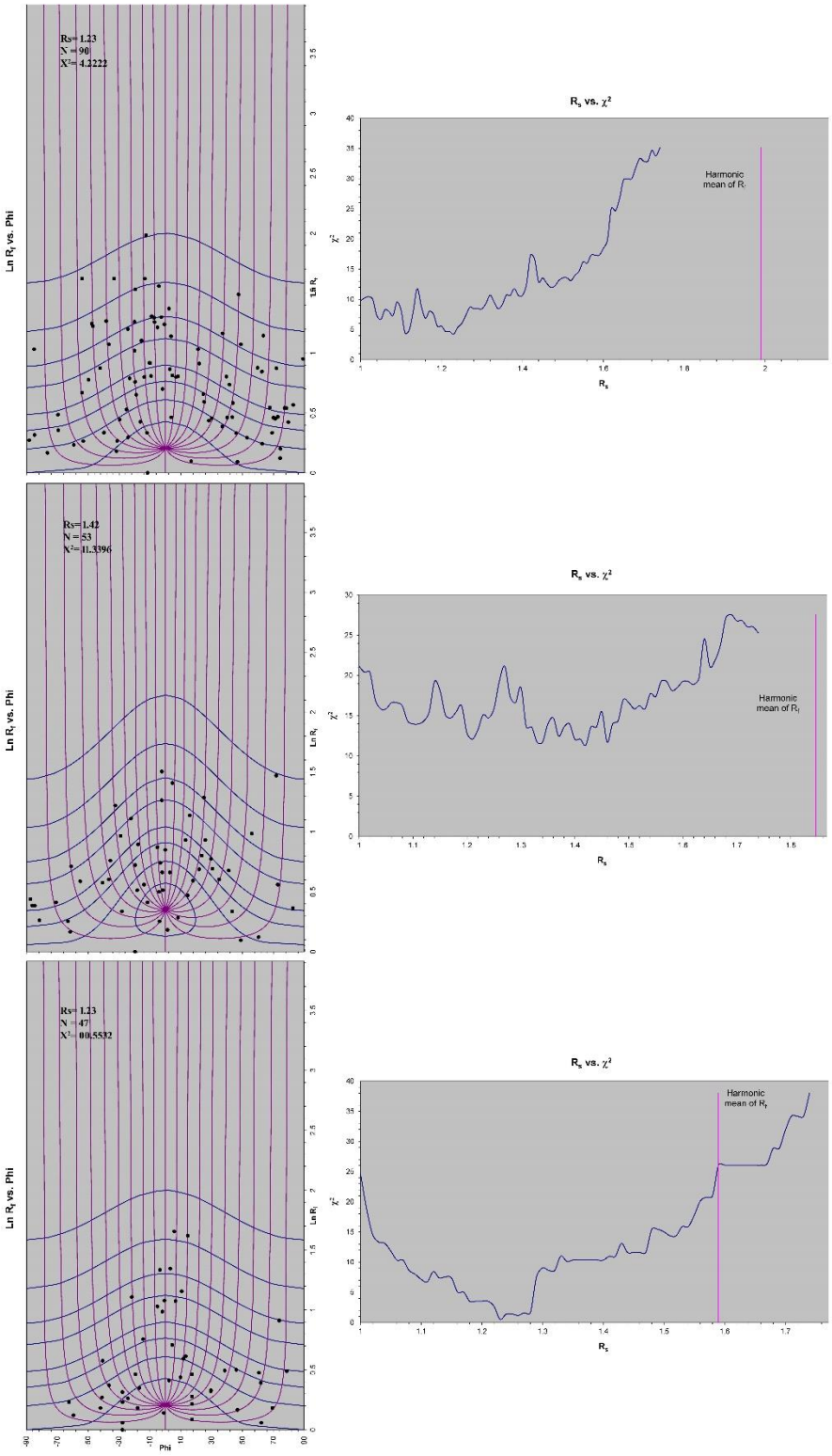


**Fig. 10. Showing the strain ratios from the *RF/φ* plots area and plotting of *Rs* vs. $X^2$ shows how the strain (*R*s) affects the best-fit parameters ($X^2$) of the θ-distribution text of three samples (10 to 12) of metavolcanic rocks (L3) in the Bir Umm Anab(LISLE, 1985).**

**Table 2. The ISYM, x2, Rs, Vector mean, Harmonic mean and Ln Harmonic mean for the studied eleven samples of metavolcanic rocks obtained from CSS.**

| Sample | $I_{SYM}$ | $x^2$ | Rs | Vector mean | Harmonic mean | Ln Harmonic mean |
|---|---|---|---|---|---|---|
| **1** | 0.7419355 | 7.35480 | 1.5 | -11.5026 | 1.8561 | 0.6185 |
| **2** | 0.8846154 | 11.0769 | 1.53 | -13.4285 | 1.7287 | 0.5474 |
| **3** | 0.9523802 | 25.4762 | 1.69 | -3.74580 | 2.0896 | 0.7370 |
| **4** | 0.8867925 | 20.3962 | 1.74 | -25.2937 | 2.2806 | 0.8245 |
| **5** | 0.8974359 | 0.3590 | 1.72 | 81.3396 | 1.8820 | 0.6324 |
| **6** | 0.8888889 | 4.0000 | 1.6 | -87.2902 | 2.3334 | 0.8473 |
| **7** | 0.7605633 | 11.9577 | 1.73 | 80.7197 | 2.1000 | 0.7419 |
| **8** | 0.8235294 | 5.2745 | 1.38 | -68.9501 | 2.1865 | 0.7823 |
| **9** | 0.7727272 | 4.4091 | 1.73 | 88.1000 | 1.9369 | 0.6611 |
| **10** | 0.7777778 | 4.2222 | 1.23 | 11.5935 | 1.9899 | 0.6881 |
| **11** | 0.8679245 | 11.3396 | 1.42 | 19.6386 | 1.8468 | 0.6135 |
| **12** | 0.8085106 | 0.5532 | 1.23 | 27.7275 | 1.5893 | 0.4633 |

scale. The metavolcanics are intruded in abundance by quartz veins that are parallel to the foliation of the host rocks and exhibit concordant aspects.

Structural analysis in the UAV indicates that the area has undergone a poly-phase structural deformation and each has its own effect and style. The deformation ranges in effects from a well-developed schistosity striking approximately E-W with dipping 60º-80º towards the south to asymmetrical folds with oblique axial planes striking into the (NNW-SSE) and dipping steeply up to 85º. The structural analysis of the veins in metavolcanic by using GArcmB software determined the paleostress inversion and displayed two clusters of veins that formed under two stresses. The stress ratios ($\Phi$)= ($\sigma 2 - \sigma 3$) / ($\sigma 1 - \sigma 3$) for both clusters, respectively, are ~0.39 and ~0.16, which distinghuishe two stress status. The values of the stress ratio on vein walls suggest that the host rock was subject to low to moderate tectonic stress at the time the veins were formed. In addition, finite strain results in metavolcanics were estimated using the Rf/φ method on deformed pebbles (with a trend of N73º-88ºE), confirming the idea that metavolcanics are affected by low to moderate deformation. The stretching mineral lineation and BIF have trend ENE-WSW to E-W that supports the oldest shortening event (D1) which is considered an early phase of deformation NNW–SSE linked with the Pan-African thrusting.

**4. References**


Abdeen, M. M., & Abdelghaffar, A. A. (2007) Post-accretionary structures in the Pan-African central Allaqi-Heiani suture zone, southeastern Egypt. J. *Geophysic. Res.* **9**.

Abdelsalam, M. G., Abdeen, M. M., Dowaidar, H. M., Stern, R. J., & Abdelghaffar, A. A. (2003) Structural evolution of the Neoproterozoic Western Allaqi–Heiani suture, southeastern Egypt. J. *Precam. Res.*, ***124** (1), 87–104.*

Baer, G., Beyth, M., & Reches, ev. (1994) Dikes emplaced into fractured basement, Timna Igneous Complex, Israel. *J. Geophysic. Res.* ***99***.

Basta, F. F., Maurice, A. E., Fontboté, L., & Favarger, P. Y. (2011) Petrology and geochemistry of the banded iron formation (BIF) of Wadi Karim and Um Anab, Eastern Desert, Egypt: Implications for the origin of Neoproterozoic BIF. *Precam. Res.* ***187***(3–4), 277–292.

Basta, F. F., Takla, M. A., & Maurice, A. E. (2000) The Abu Marawat banded iron formation: geology, mineralogy, geochemistry and origin. *5th International Conference on the Geology of the Arab World*, 319–334.

Chew, D. M. (2003) An Excel spreadsheet for finite strain analysis using the Rf/φ technique. *Computers and Geosciences*, *29*(6), 795–799.

Delaney, P. T., Pollard, D. D., Ziony, J. I., & McKee, E. H. (1986) Field relations between dikes and joints: Emplacement processes and paleostress analysis. *J. Geophysi. Res.* ***91***, 4920–4938.

Dixon, T. H. (1979) *Evolution of continental crust in the Late Precambrian Egyptian Shield*. California Univ., San Diego (USA).

Dunnet, D. (1969) A technique of finite strain analysis using elliptical particles. *Tectonophysics*, ***7*** (2), 117–136.

El Habaak, G. H., & Soliman, M. F. (1999) Rare earth element geochemistry of the Egyptian banded iron formations and the evolution of the Precambrian atmosphere and ocean. *4th International Conference on Geochem.*, 149–160.

El-Gaby, S., Khudeir, A., El-Habbak, G., & El-Aref, G. (1993) Geology and genesis of Wadi Kareim banded iron formation. In H. Schandelmeier & U. Thorweihe (Eds.), *Geoscientific Research in Northeast Africa*. CRC Press.

El-Ramly, M. F. (1972) A new geological map for the basement rocks in the Eastern and Southwestern Desert of Egypt, scale 1:1000 000. *Ann. Geol Surv. Egypt*, ***2***, 1–18.

El-Tokhi, M., Alaabed S., & Amin, B (2010) Late Precambrian metavolcanics of Um Anab North Eastern Desert, Egypt, geochemistry and tectonic environment studies. *Eur. J. Sci. Res.*, **42** (3), 507-524.

Eyles, N., & Januszczak, N. (2004) 'Zipper-rift': a tectonic model for Neoproterozoic glaciations during the breakup of Rodinia after 750 Ma. *Earth-Science Reviews*, ***65*** (1–2), 1–73.

Gharib, M. E., Maurice, A. E., & Selim, H. A. (2021) Tonian/Cryogenian Island Arc Metavolcanics of the Arabian-Nubian Shield. *The Geology of the Arabian-Nubian Shield*, 267-296.

Greiling, R. O., Abdeen, M. M., Dardir, A. A., El Akhal, H., El Ramly, M. F., El Din Kamal, G. M., ... & Sadek, M. F. (1994) A structural synthesis of the Proterozoic Arabian-Nubian Shield in Egypt. Geol. Rundsch. **83**, 484-501.

Hamimi, Z., El-Fakharani, A., & Abdeen, M. M. (2014) Polyphase deformation history and strain analyses of the post-amalgamation depositional basins in the Arabian–Nubian Shield: Evidence from Fatima, Ablah and Hammamat Basins. *J. Afric. Earth Sci.* ***99*** (PA1), 64–92.

Hamimi, Z., El-Wahed, M. A., Gahlan, H. A., & Kamh, S. (2018) Tectonics of the Eastern Desert of Egypt: Key to Understanding the Neoproterozoic Evolution of the Arabian–Nubian Shield (East African Orogen). *The Geol. Arab World—An Overview*.

Hashad, A. H. (1978) Present status of geochronological data on the Egyptian basement complex. *Precam. Res*. ***6***, 31–46.

Johnson, P. R., & Woldehaimanot, B. (2003) Development of the Arabian-Nubian Shield: perspectives on accretion and deformation in the northern East African Orogen and the assembly of Gondwana. *Geol. Soci. London, Spec. Public.* ***206*** (1), 289–325.

Jolly, R. J. H., & Sanderson, D. J. (1997) A Mohr circle construction for the opening of a pre-existing fracture. *J. Struc. Geol.* ***19*** (6), 887–892.

Kassem. O. M.. Rahim. S. H. A. E.. & Nashar. E. S. R. E. (2012) Strain analysis and microstructural evolution characteristic of Neoproterozoic rocks associations of Wadi El Falek, Centre Eastern Desert, Egypt. *Geotectonics*, ***46*** (5), 379-388.

Koehn. D.. Arnold. J.. & Passchier. C. W. (2005) Fracture and vein patterns as indicators of deformation history: a numerical study. *Geol. Soci. London, Spec. Public.* ***243*** (1), 11-24.

Kroner, A. (1984) Late Precambrian plate tectonics and orogeny: A need to redefine the term Pan-African. In J. Klerkx & J. Michot (Eds.), *Geologic Africaine* (pp. 23–28). Tervuren,.

Kröner, A. (1991) Tectonic evolution in the Archaean and Proterozoic. *Tectonophysics*, ***187***(4), 393–410.

Kusky, T. M. Abdel Salam, M. G., Stern, R. J., & Tucker, R. D. (2003) Evolution of the East African and related orogens, and the assembly of Gondwana. J. *Precam. Res*. ***123*** (2–4), 81–340.

Lisle J. R. (1985) Geological Strain Analysis (First Edition). Pergamon Press, Oxford.

Love J. J. (2007) Bingham Statistics. In Gubbins David & Herrero-Bervera Emilio (Eds.), *Encyclopedia of Geomagnetism and Paleomagnetism* (pp. 45–47). Springer Dordrecht.

Meneisy, M. Y. (1990) Volcanicity. In Said R. (Ed.), *The Geology of Egypt* (pp. 157–174). Balkema, Rotterdam.

Mulchrone, K. F., & Meere, P. A. (2001) A Windows program for the analysis of tectonic strain using deformed elliptical markers. *Computers & Geosciences*, ***27*** (10), 1251–1255.

Mulchrone, K. F., Meere, P. A., & Choudhury, K. R. (2005). SAPE: A program for semi-automatic parameter extraction for strain analysis. *J. Struc. Geol.* ***27*** (11), 2084–2098.

Mulchrone, K. F., O'Sullivan, F., & Meere, P. A. (2003) Finite strain estimation using the mean radial length of elliptical objects with bootstrap confidence intervals. *J. Struc. Geol.* ***25*** (4), 529–539.

Passchier, C. W., & Trouw, R. A. (2005) Microtectonics. *Springer Science & Business Media. Berlin*.

Ramsay, J. G., Huber, M. I., & Lisle, R. J. (1983) The techniques of modern structural geology: Folds and fractures (***Vol. 2***). *Academic press*.

Ries, A. C., Shackleton, R. M., Graham, R. H., & Fitches, W. R. (1983) Pan-African structures, ophiolites and mélange in the Eastem Desert of Egypt: a traverse at 26°N. *J. Geol. Soci.* ***140*** (1), 75–95.

Stein, M., & Goldstein, S. L. (1996) From plume head to continental lithosphere in the Arabian–Nubian shield. *Nature*, ***382***(6594), 773–778.

Stern, R. J. (1981) Petrogenesis and tectonic setting of late Precambrian ensimatic volcanic rocks, central eastern desert of Egypt. J. *Precam. Res*. ***16*** (3), 195–230.

Stern, R. J. (1994) Arc assembly and continental collision in the neoproterozoic East African Orogen: Implications the Consolidation of Gondwanaland for. In *Annu. Rev. Earth Planet. Sci.* **22**.

Stern, R. J., & Hedge, C. E. (1985) Geochronologic and isotopic constraints on late Precambrian crustal evolution in the Eastern Desert of Egypt. *American Journal of Science*, ***285***(2), 97–127.

Wallbrecher, E. (2012) Fabric8: A Program Package for Graphical Display and Analysis of Tectonic Data.

Yamaji, A. (2016) Genetic algorithm for fitting a mixed Bingham distribution to 3D orientations: A tool for the statistical and paleostress analyses of fracture orientations. *Island Arc*, ***25*** (1), 72–83.

Yamaji, A., & Sato, K. (2011) Clustering of fracture orientations using a mixed Bingham distribution and its application to paleostress analysis from dike or vein orientations. *J. Struc. Geol.* ***33*** (7), 1148–1157.

Yamaji, A., Sato, K., & Tonai, S. (2010) Stochastic modeling for the stress inversion of vein orientations: Paleostress analysis of Pliocene epithermal veins in southwestern Kyushu, Japan. *J. Struc. Geol.* ***32*** (8), 1137–1146.

# الدراسات الجيولوجية والتحليل الإنشائي للبركانيات المتحولة بمنطقة أم عناب وعروق الكوارتز بها: الآثار المترتبة على النشاط البركاني الأفريقي في الدرع النوبي المصري

**خالد الجميل[١]، سارة فايد[١]،حمدي الدسوقي[٢]، أشرف عبد المقصود[١]**

[١]قسم الجيولوجيا، كلية العلوم، جامعة المنوفية

[٢]برنامج جيولوجيا البترول والتعدين، كلية العلوم، جامعة الجلالة الأهلية

تقع صخور القاعدة ذات أعمار النيوبروتيروزويك في منطقة أم عناب على بعد ٤٠ كم جنوب غرب مدينة الغردقة في الصحراء الشمالية الشرقية (NED) من مصر. تشتمل صخور القاعدة فى المنطقة على بركانيات متحولة وبلوتونات ضخمة من صخور الجرانيت. تظهر الصخور البركانية تحولًا إقليميًا يصل الى سحنات الشيست الاخضر او الامفيبوليت. تظهر تتابعات الصخور البركانية مقحمة مع تكوينات الحديد الشرائطى (BIF) فى وضع متبادل. يشير التحليل الإنشائي في بركانيات أم عناب (UAV) إلى أن المنطقة بها تشوه بنيوي متعدد الأطوار ، ولكل منها تأثيرها وأسلوبها الخاص. وقد لاحظ وجود أنسجة وتراكيب شستية متطورة تتجه شرق–غرب مع ميل ٦٠–٨٠ درجة نحو الجنوب، وطيات غير متماثلة ذات مستويات محورية مائلة بزاوية مائلة تصل إلى ٨٥ درجة. حدد التحليل الهيكلي لعروق الكواريز في الصخور البركانية باستخدام برنامج GArcmB عكس الإجهاد القديم وعرض عدد من العروق التي تشكلت تحت ضغطين. نسبة الإجهاد (σ1 – σ3) / (σ2 – σ3) = (Φ) لكلا العقد، على التوالي، هي ~ ٠,٣٩ و ~ ٠,١٦، مما يوضح وجود حالتين من الإجهاد. تشير قيم نسبة الإجهاد على جدران العروق إلى أن الصخور المضيفة تعرضت لإجهاد تكتوني منخفض إلى معتدل في وقت تشكل العروق. بالإضافة إلى ذلك، تم تقدير نتائج التشوه النهائي في الصخور البركانية باستخدام طريقة Rf / φ على الحبيبات المشوهة والموجهة ذات اتجاه N73º–88ºE ، مما يؤكد فكرة أن الصخور البركانية القديمة تتأثر بالتشوه المنخفض إلى المعتدل. تتجه خطوط المعادن الممتدة وتشكيلات خام الحديد باتجاه شرق–شمال شرق إلى غرب–جنوب غرب، مما يدعم أقدم حدث تشوه حدث الأختزال (D1) الذي يعتبر مرحلة مبكرة من التشوه شمال غرب – جنوب شرق والمرتبط بالحركات التكتونية البان–أفريقية.